EARTH SCIENCES
RESEARCH JOURNAL
Earth Sci. Res. J. Vol. 29, No. 1 (March, 2025): 23 - 33

UNIVERSIDAD NACIONAL DE COLOMBIA

ORE GEOLOGY

The sedimentary environment and source of ore-forming materials of sandstone-type copper deposits in southeast Kuqa Basin, Xinjiang, China

Qiji Fu, Xinxian Xu*
Hainan Survey Institute of Mineral Resources, Haikou 571100, China
* Corresponding author: llj201260030@ecut.edu.cn

ABSTRACT

A series of sandstone-type copper deposits and occurrence distribute in the Kuqa Basin, Xinjiang. Based on field surveys, we carried out research into the sedimentary environment and metallogenic model of copper deposits southeast of the basin. The relationship between the sedimentary environment/facies in the area and the copper mineralization were summarized to explore the genesis of mineralization and the metallogenic model. We identified main sedimentary facies types of alluvial fans, fan deltas, and lakes in the Neogene strata, and further identification of five subfacies and seven microfacies were made. Our research results reveal that the genesis of sandstone-type copper mineralization is related to the sedimentary environment, and the mineralized bodies are mainly distributed in fan delta plain facies and fan delta front facies. Detrital zircon dating results of two samples from Kangcun area are 427.4 ± 6.6 Ma, 387.3 ± 3.3 Ma and 424.6 ± 2.3 Ma, 279.9 ± 6.8 Ma.The other two samples from Duwanke area are 285.6 ± 3.0 Ma, 449.5 ± 3.2 Ma and 427.5 ± 2.3 Ma. It indicates that the source of the copper-bearing sandy conglomerate in the Miocene Jidike Formation (N_1j) is mainly from the strata and magmatic rock products formed by the geological evolution during the Late Silurian to Early Permian

Keywords: Kuqa Basin; sandstone-type copper deposit; LA-ICP-MS; sedimentary environment

Entorno sedimentario y fuente de materiales formadores de minerales de depósitos de cobre tipo arenisca en el sureste de la cuenca de Kuqa, Xinjiang, China

RESUMEN

Una serie de depósitos y ocurrencias de cobre de tipo arenisca se distribuyen en la cuenca de Kuqa, Xinjiang. Basado en observaciones de campo los autores realizaron esta investigación del ambiente sedimentario y del modelo metalogénico de los depósitos de cobre en sureste de la cuenca. La relación ambiente/facies sedimentaria en el área y la mineralización cuprífera fueron sintetizada para explorar el origen de los modelos de mineralización y metalogenia. Los autores identificaron los principales tipos de facies sedimentarias de los abanicos aluviales, deltas en abanico y lagos en los estratos neógenos, y se realizó una identificación adicional de cinco subfacies y siete microfacies. Los resultados de la investigación revelan que el origen de la mineralización cuprífera tipo arenisca se relaciona con el ambiente sedimentario y que los cuerpos mineralizados se distribuyen principalmente en facies de llanura deltaica y facies de frente deltaico. Los resultados de datación con circón detrítico de dos muestras del área de Kangcun presentan los rangos de 427.4 ± 6.6 Ma, 387.3 ± 3.3 Ma y 424.6 ± 2.3 Ma, 279.9 ± 6.8 Ma. Las otras dos muestras del área de Duwanke estan entre 285.6 ± 3.0 Ma, 449.5 ± 3.2 Ma y 427.5 ± 2.3 Ma. Esto indica que la fuente del conglomerado arenoso de contenido cuprífero en la formación Jidike del Mioceno proviene principalmente de los estratos y productos de roca magmática formados por la evolución geológica durante el Silúrico Tardío al Pérmico Temprano.

Palabras clave: Cuenca Kuqa; depósitos cupríferos de tipo arenisca; ambiente sedimentario.

Record
Manuscript received: 03/12/2024
Accepted for publication: 10/03/2025

How to cite item:
Fu, Q., & Xu, X. (2025). The sedimentary environment and source of ore-forming materials of sandstone-type copper deposits in southeast Kuqa Basin, Xinjiang, China. *Earth Sciences Research Journal, 25*(1), 23-33. https://doi.org/10.15446/esrj.v29n1.117846

Introduction

The Tarim Basin is a metallogenic and exploration area for the coexistence of important metal minerals, coal, and oil resources in China (Lin C S et al., 2002, Cao Y T, 2010, Zhao M J et al., 2015, Fang W X et al., 2016, Xiao Y, 2018, Lu K G et al., 2019, Zhang T et al., 2020), which became a hot spot in the study of tectonic evolution and metallogenic laws in recent years (Liu Z H et al., 2000, Yan F L et al., 2003, Tang L J et al., 2004, Charreau J et al., 2006, Cao Y T, 2010, Guan S W et al., 2010, Li X et al., 2013, Cai H A et al., 2022, Cai H A, 2023). The sedimentary development of Mesozoic terrigenous clastic rocks in the study area is relatively complete, and the sedimentary characteristics of foreland basins are obvious (Jia C Z et al., 1995). Scholars have conducted detailed studies on the structure (Qian J F et al., 2012, Lu K G et al., 2019), sequence (Guo X P et al., 2002, Lin C S et al., 2002, Shao L Y et al., 2007), sedimentary environment (Li J F et al., 2017) and paleogeography (Shao L Y et al., 2006, Tan X C et al., 2006). There are a series of sandstone-type deposits and occurrences in the Cenozoic strata in the Kuqa Basin, such as the Dishui copper mine (Liu D Q et al., 2005). However, the relationship between sandstone-type copper deposits and the source-sink system of sedimentary basins needs to be further studied.

In recent years, more and more isotopic dating of zircon in clastic rocks has been applied to the study of basin provenance and craton geological evolution (Wu F L and Yao Z G, 2011, Hu B et al., 2013). Therefore, based on field investigation, this paper tests the age of volcanic clastic zircon in the copper-bearing conglomerates of the Miocene Jidike Formation(N_1j), which provides chronological evidence for the study of the relationship between sandstone-type copper deposits and the source-sink system of sedimentary basins, and provides a theoretical basis for future exploration work in this area. At the same time, the record of geological events preserved by detrital zircon in clastic rocks also provides important evidence for the geological evolution of the Tarim Craton.

1. Geological background

There is a copper ore belt with a length of 1000 km and a width of 15~70 km in the northern margin of Tarim (Fig. 1a). The zone is composed of Paleogene and Neogene fluvial-lacustrine sediments. The copper-bearing sandstone-type copper sources are concentrated in the Paleogene of the Kuqa Basin and the Wucha Basin (Liu D Q et al., 2005). Among them, the Kuqa Basin has undergone 3 stages of tectonic movement (Liu Z H et al., 2000), and the Neogene-Quaternary tectonic movement has formed a large thrust fold system and a series of thrust faults in front of the Tianshan Mountains (Zhang M L et al., 2004). It has the structural characteristics of "north-south zone, east-west section, upper and lower layering". The copper metallogenic belt is mainly located in the Qiulitag anticline tectonic zone (Fig. 1a). The outcropping strata in the area are Neogene and Quaternary, and sandstone-type copper deposits are produced in Neogene strata. Among them, the Miocene Jidike Formation (N_1j) and Kangcun Formation (N_1k) are ore-bearing horizons with relatively stable production (Fig. 1b), while the Upper Miocene Kuqa Formation only occasionally occurs copper mineralization at the sandstone and mudstone interface. The Miocene Gidiq Formation (N_1j) is a set of continental clastic rocks of the delta front, mainly interbedded with gray-green conglomerate, purple-red, brown-red mudstone and sandy mudstone, interbedded with a small amount of light purple-red sandstone, with a thickness of 300~840 m, and the upper part is marked by a gypsum layer and gray-green argillaceous siltstone at the top, and copper mineralization is common in the coarse clastic rocks of this formation (Fig. 2a), mostly in a layered distribution (Fig. 2b). The Kangcun Formation (N_1k) is a set of continental clastic sediments on the delta front, mainly gray-green mudstone and sandy mudstone interbedded with a small amount of gray-green mudstone and sandy mudstone, interbedded with gray conglomerate and argillaceous medium-coarse-grained sandstone, etc., with cross-bedding (Fig. 2c) and occasional traces of bioturbation (Fig. 2d), which can be further subdivided into the first member of the Kangcun Formation and the second member of the Kangcun Formation. The first member of the Kangcun Formation (N_1k^1) is mainly interbedded with light reddish-brown mudstone and medium-thin bedded gray-green sandstone, with occasional fading and alteration at the boundary (Fig. 2e), which is a favorable site for copper mineralization, among which there are many interbeds of local gray-dark gray thick-bedded conglomerate, interspersed with gypsum network veins (Fig. 2f), and multi-layered thin-bedded copper mineralization is found in coarse sandstone, mainly manifested as chalcochlorite and malachite (Fig. 2g, 2h). The second member of the Kangcun Formation (N_1k^2) is mainly earthy yellow mudstone with a small amount of thin-bedded sandstone, with a thickness of 205~540 m. The Kuqa Formation (N_2k) is a set of continental clastic deposits, with a lithology dominated by gray-dark gray, brown, and a small amount of yellow-green coarse-boulder conglomerate, interbedded with sandy mudstone, argillaceous medium-coarse sandstone, etc. (Fig. 2i), which is in integrated contact with the under kangcun Formation.

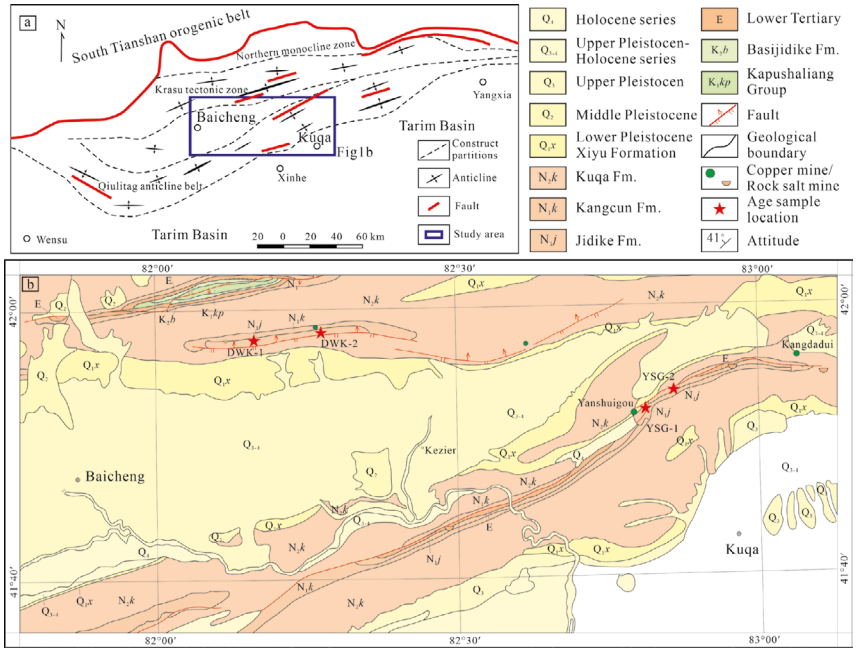

Figure 1. Maps showing the structural zoning and copper deposits distribution in the Kuqa Basin and a simplified geological map of the Kangcun area (a) Structural zoning map of the Kuqa Basin (Li X et al., 2013); (b) Simplified geological map of the study area

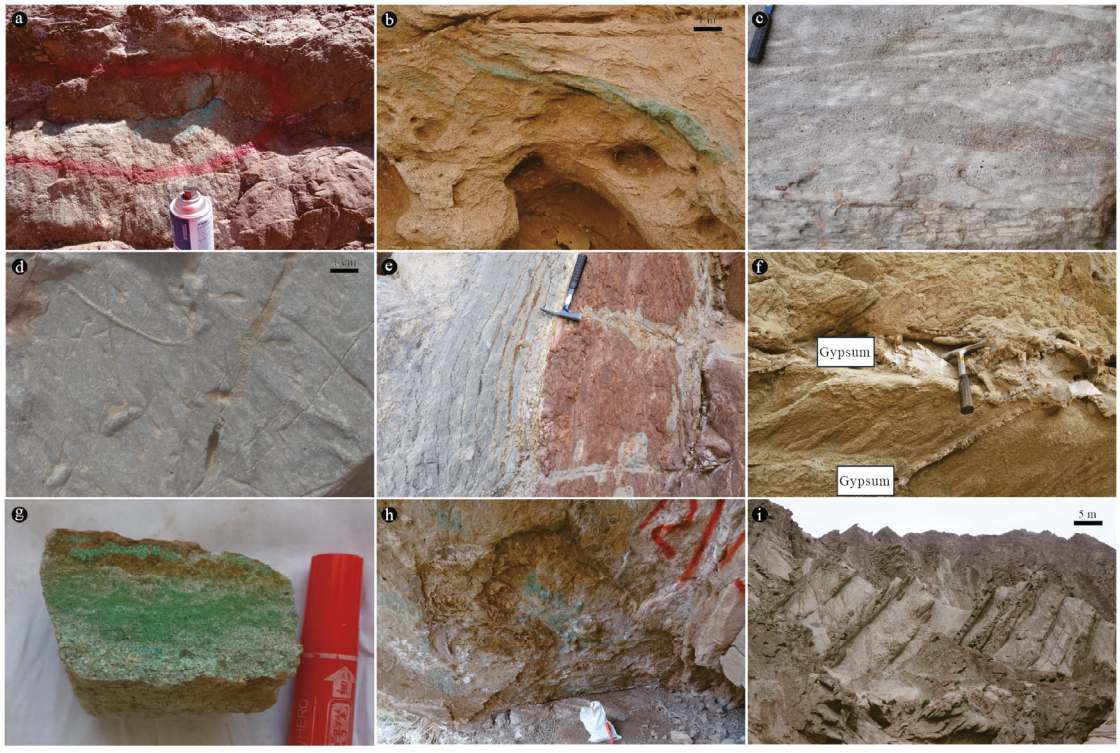

Figure 2. Field outcrops of the sandstone-type copper deposits in the southeast Kuqa Basin (a) Copper mineralization in conglomerates of the Jidike Formation; (b) Copper mineralization in coarse sandstones of the Jidike Formation; (c) Cross bedding in coarse sandstone of the Kangcun Formation; (d) Bioturbation traces in argillaceous sandstones of the Kangcun Formation; (e) Fading alteration in sandstones of the Kangcun Formation; (f) Coarse sandstones crossed by gypsum veins in the Kangcun Formation; (g) Hand specimen of ore body in the Kangcun Formation; (h) Copper deposits at the interface between sandstone and mudstone in the Kangcun Formation; (i) Sandstone and mudstone interbedding in the Kuqa Formation

2 Sandstone-type copper sedimentary environment in the Kuqa Basin

The Kuqa Basin is a regenerated foreland basin (Yan F L et al., 2003), and the Triassic foreland basin underwent Mesozoic basin extension, Late Cretaceous extrusion, uplift and denudation, and was revived in the Cenozoic after Paleocene transgression (Jia C Z et al., 1995, Qian J F et al., 2012), at which time a set of continental clastic sediments were deposited in the Kuqa Basin that were denuded by the uplift of the Tianshan orogenic belt (Yang G and Qian X L, 1995). During the Miocene, the Tianshan Orogenic Belt on the northern margin of the foreland basin was uplifted rapidly, and the topographic elevation difference was very different, with alluvial fan-braided fluvial deposits in the piedmont zone, alluvial fans in the Jidike Formation, and fluvial alluvial plains in the south (Tian Z J and Song J G, 1999). The ore-bearing rocks in the Kangcun area are the Jidike Formation (N_1j) and the first member of the Kangcun Formation (N_1k^1), which are a set of stably distributed variegated clastic deposits such as purple-red, brown-red, gray-green, and dark gray, with relatively developed sedimentary structures and little change in thickness.

2.1 Sedimentary petrology characteristics

The lithologic assemblage of the Jidike Formation (N_1j) in the study area is dominated by gray-green conglomerate, brown-red sandy mudstone, interbedded with a small amount of light purple-red sandstone, which is a set of continental clastic sediments at the delta front. The lithologic assemblage of the Kangcun Formation (N_1k) is dominated by earthy yellow, light purple-red interspersed with a small amount of gray-green mudstone and sandy mudstone, interbedded with gray conglomerate, argillaceous medium-coarse-grained sandstone, etc., which is a set of continental clastic deposits of the delta front. The lithology of the Kuqa Formation (N_2k) is mainly gray-dark gray, brown, with a small amount of yellow-green coarse-boulder conglomerate, interbedded with sandy (conglomerate) mudstone, argillaceous medium-coarse sandstone, etc. (Fig. 2i), which is in integrated contact with the under Kangcun Formation and is a set of continental clastic deposits.

2.2 Sedimentary structures

The field investigation found that various sedimentary structures such as bedding structures and layer structures were developed in the Neogene strata in the study area: cross-bedding and undulating bedding were common bedding structures in the strata in the study area (Fig. 2c), and the common layer structures included wave marks and bottom scouring structures.

2.3 Paleontological characteristics

The content of biological fossils in the area is very low, and only a small number of fossils from biological caves are found in the field (Fig. 2d), which are commonly found in siltstone and argillaceous siltstone.

2.4 Sedimentary system division and characteristics

The Neogene sedimentary systems in the Kangcun area of the Kuqa Basin are mainly alluvial fan-fan delta and lacustrine (Fig. 3a), and the main sedimentary facies types can be identified as alluvial fan-delta facies and lacustrine facies (Fig. 3b-3d), and five subfacies and seven microfacies types can be identified (Fig. 1). The main sedimentary facies characteristics are described below.

2.4.1 Alluvial fan facies

The alluvial fan facies in the Kangcun area are concentrated in the Kuqa Formation and the Quaternary, which reflects that the survey area is arid with less precipitation, and the temporary foothill torrent develops and forms at the

mouth of the valley (Fig. 3b). The Kuqa Formation in the area is a set of coarse clastic assemblages with typical alluvial fan facies characteristics, and the lower part is gray conglomerate upward to gray massive conglomerate and coarse conglomerate interbedded, and occasionally coarse sandstone lenses with oblique bedding development.

2.4.2 Fan delta facies

The important conditions for the development of fan delta are the large terrain elevation difference near the shore of the impoundment body, the steep and narrow slope on the shore, and the sufficient supply of detrital materials near the source. The study area is mainly distributed in the strata of the Jidike Formation and the Kangcun Formation (Figs. 3b and 3c), which is dominated by mudstone and locally interbedded with thin-bedded siltstone, with horizontal bedding and wave-forming sand-grained bedding in siltstone. It can be subdivided into fan delta plain subfacies, fan delta front subfacies and forefan delta subfacies.

(1) Fan delta plain subfacies

The subfacies of the fan delta plain is characterized by the development of coarse clastic rocks, the bedding is not developed, and the sorting and roundness are poor. In the Kangcun area, the subfacies can be subdivided into two microfacies, the former is mainly composed of conglomerate, coarse sandstone and a small amount of siltstone, and the bedding includes granular sequence bedding, parallel bedding and cross-bedding (Fig. 2c), and the latter is composed of mudstone and thin-bedded siltstone, with horizontal bedding and a small amount of cross-bedding. The subfacies zone of the fan delta plain is mainly concentrated in the Kangcun Formation (Fig. 3c).

(2) Fan-delta front subfacies

The subfacies of the fan delta front is the sedimentation of the underwater part of the fan delta, which is usually located in the shallow water between the shoreline and the wave base. In the Kangcun area, it can be subdivided into underwater distributary channel microfacies, underwater distributary channel microfacies, estuarine sand bar microfacies and leading mat sand microfacies. The sediments of the underwater distributary channel have medium-to-small crossbedding, oblique bedding and bottom scouring structures, and the estuarine sand bars have antigranular sequence and cross-bedding. The microfacies between the underwater distributary channels in the area is mainly composed of mudstone and siltstone, with a small amount of fine sandstone, and horizontal bedding is developed. The mat sand microfacies sediments at the front edge have finer grain size and better sorting, and small cross-bedding and undulating bedding are developed. The subfacies zone of the fan-delta front margin is mainly concentrated in the Jidik Formation and the Kangcun Formation (Figs. 3c, 3d).

(3) Front fan-delta subfacies

It is in a deep-water area below the wave base plane, and the lithological assemblage is mudstone and thin-bedded siltstone, and the horizontal bedding is developed. The subfacies is underdeveloped in the Kangcun area, with a small and discontinuous area, and the lithological assemblage is mudstone and siltstone, and the overall grain sequence is coarse upward.

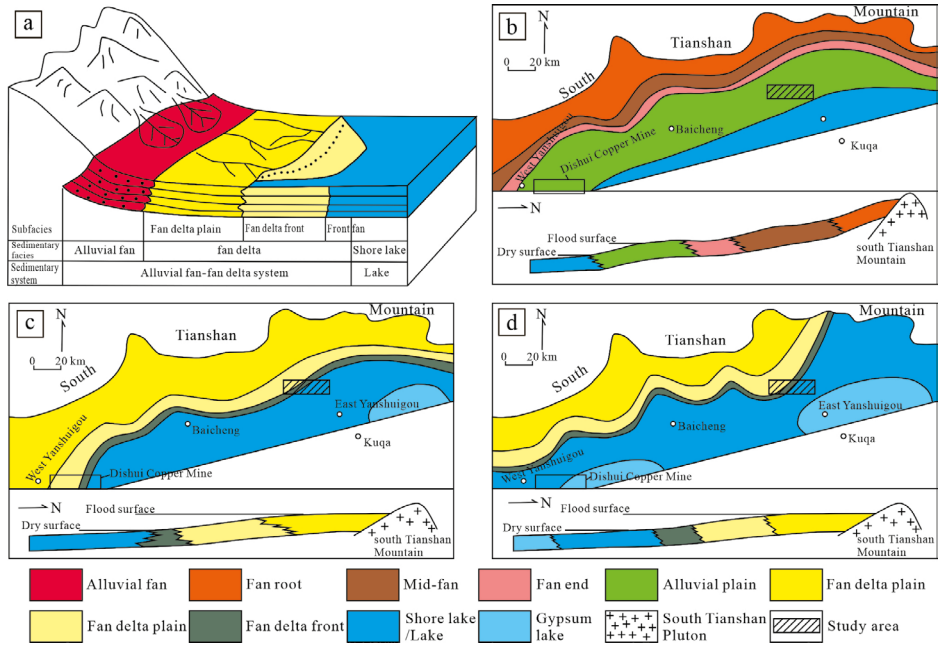

Figure 3. Sedimentary facies model and distribution of sedimentary facies in the Kuqa Basin since the Neogene (Li X et al., 2013; Shi W G et al., 2015) (a) Diagram showing the sedimentary mode of alluvial fan-fan delta-lake; (b) Distribution of sedimentary facies in the Kuqa Formation; (c) Distribution of sedimentary facies in the Kangcun Formation; (d) Distribution of sedimentary facies in the Jidike Formation

Table 1. Division of sedimentary facies in the Kangcun area, Kuqa foreland basin

Sedimentary system	Sedimentary facies	Subfacies	Microfacies	Distribution Strata
Terrestrial sedimentary system	Alluvial fan facies			N_2k, Q
	fan delta facies	Fan delta plain	Distributary channel, Diversion bay	
		Fan delta front	Underwater diversion channels, between underwater distributary channels, estuary sandbar, Front edge sheet-like sand	N_1j, N_1k
		Front fan delta		
	Lake facies	Shore lake		N_1j, N_2k
		Gypsum lake	Gypsum sedimentation	

2.4.3 Lake facies

It is mainly distributed in the southern part of the study area (Fig. 3d), represented by thick-bedded mudstone gypsum rocks, which can be divided into shallow lake subfacies and gypsum lake subfacies, and the lacustrine facies in the study area generally has a southward shrinking trend since the Paleogene.

3 Discussions

3.1 Characteristics of copper orebody and its relationship with sedimentary facies configuration

The overall characteristics of copper mineralization in the study area are obviously controlled by stratigraphy, which are mainly concentrated in the Miocene Jidike Formation and the first member of the Kangcun Formation. Copper mineralization is dotted and disseminated in gray-white (gravel) coarse sandstone, mainly along the interlayer or nearly vertical layer of sand and mudstone, and the interlayer and joint surface are filled with salt and gypsum, and the copper mineral is impregnated to the surface of gypsum and salt, with a small thickness but a large intermittent extension. Copper minerals include chalcochlorite, malachite, azurite and bornite, and the surrounding rock alteration is not developed, which is a sedimentary origin of sand type copper mineralization, and local copper mineralization enrichment areas can be mined. Field observations and laboratory studies have identified four mineralized bodies of varying sizes, all of which are more than 100 m in length, three of which are over 500 m in length, and vary in thickness from 5 cm to 2.4 m (Fig. 1b).

In the early Neogene Giddic period, the lake shrank to the south, mainly in the fan delta and lacustrine sediments; in the Kangcun period, the sedimentary pattern of the Gidiq period was basically inherited, the fan delta area expanded, the lake area shrank to the south, and the piedmont to the basin was a fan delta to lake sedimentation; in the Kuqa period, alluvial fans mainly developed in the piedmont, and alluvial fan facies, alluvial plain facies and lacustrine facies were developed from north to south; in the Quaternary the lakes disappeared, alluvial fan sediments were mainly developed (Fig. 3; Li X et al., 2013). The genesis of sandstone-type copper mineralization is closely related to the sedimentary environment of Neogene fluvial-lacustrine facies, and the minerals are mainly distributed in the fan-delta plain facies and fan-delta front facies. On the one hand, it is due to the development of the porosity of coarse clastic sedimentary rocks, which is conducive to the enrichment of copper-bearing materials, while coarse clastic sediments are often developed in places with strong hydrodynamics. In addition, sandstone-type copper mineralization is often related to the oxidation-reduction chemical phase at the time of formation, and the mineralized bodies observed in the field are mostly produced on the side of the light-colored layer at the junction of light-colored clastic rocks and purple-red clastic rocks, which represents the initial source layer of the oxidized geochemical facies purple-red layer, and the light-colored layer of the reducing geochemical facies is the place where minerals accumulate during diagenesis or metagenesis. This oxidation-reduction chemical phase is generally found at the junction of rivers and lakes, that is, at the junction of rivers and lakes that represent the oxidizing environment. This phenomenon is like that of Dishui Copper (Shi W G et al., 2015; Fig. 3). Combined with the geophysical and geochemical anomalies and the surface verification results, the three prospecting prediction areas (Fig. 1b) are all distributed at the junction of rivers and lakes centered on the Jidik Formation.

3.2 Provenance evolution of ore-bearing conglomerates in the Gidik Formation

The provenance zone is one of the key factors for the characteristic change of sediments in the basin. The Kangcun area is located at the intersection of multiple provenance systems, and the Paleogene-Neogene sedimentary system is complex and changeable. From the perspective of the tectonic position of the study area, the South Tianshan Mountains and the Wensu Bulge were the main sediment supply sources in this period, and they were the main source supply areas in the study area during the Neogene Jidik-Kangcun period (Jia C Z et al., 1995, Qiu F Q et al., 2000, Li Z et al., 2004, Li S J et al., 2006). Qiu F Q et al. (2000) quantitatively analyzed the skeletal mineral composition of the sandstone, and concluded that the Cretaceous-Paleogene source area in the Kuqa Basin was mainly the result of denudation and redeposition of the Carboniferous strata in the southern margin of the South Tianshan Mountains and the Silurian-Devonian strata in the South Tianshan Mountains. Li Z et al. (2004) compared and analyzed the clastic assemblage and regional climate change events in the Kuqa Basin and the time of tectonic uplift in the Tianshan region, and suggested that the clastic rocks of the Miocene Jidik-Kangcun Formation, especially the Upper Miocene Kuqa Formation, may be the result of the superposition of tectonic uplift and frequent climate changes in the Tianshan Mountains. Li S J et al. (2006) systematically analyzed the characteristics of heavy mineral content in the sandstone of Kuqa Basin, and concluded that the large-scale uplift and denudation of the South Tianshan Mountains occurred since the Paleogene, because its uplift obscured the material contribution of the Paleozoic accretion complex on the northern margin of the South Tianshan Mountains.

In order to study the provenance zone and age of the mineral-bearing conglomerate in the Jidike Formation, two copper-bearing conglomerate age samples were collected in the area of Yanshuigou in the Kangcun area, numbered YSG-1 and YSG-2, respectively (Fig. 1b). The sample was crushed to below 60 mesh (250 μm), the zircon was coarsely separated by magnetic separation and heavy liquid method, and the zircon particles were picked out under the microscope. The zircon particles are fixed in transparent epoxy resin for grinding and polishing. Cathodoluminescence photography of the polished zircon shows that the shape of the zircon is sub-circular and sub-angular, most of which remain more self-shaped prismatic, and most of them are magmatic zircon with oscillating rings. Cathodoluminescence photography and zircon U-Pb isotope testing was done at the State Key Laboratory of Continental Dynamics at Northwest University. The U-Pb isotopic age was measured by Agilent7500a laser ablation inductively coupled plasma mass spectrometry (LA-ICP-MS), and the results of cathodoluminescence irradiation, analysis points and test results are shown in Figures 4 and 5. The YSG-1 samples measured the harmonic ages of many groups, among which 427.4 ± 6.6 Ma and 387.3 ± 3.3 Ma harmonics were better, and the YSG-2 samples also measured the harmonic ages of many groups, among which 424.6 ± 2.3 Ma and 279.9 ± 6The age harmony between the two groups was better at 8 Ma. The detrital zircon dating statistics show the distribution peaks of 427 Ma and 424 Ma in the Early Paleozoic, corresponding to the zircon formed by the Late Silurian magmatic activity, 387 Ma corresponding to the zircon formed by the Middle Devonian magmatic activity, and the 280 Ma distribution peak, corresponding to the zircon formed by the early Permian magmatic activity in the Late Paleozoic.

The Halke Mountain intrusive rocks in the southwest Tianshan Mountains are dominated by Silurian intrusive rocks, followed by Carboniferous intrusive rocks, and the lithology is dominated by diorite. Liu B P et al. (1996) measured the Ping age of the Silurian intrusive amphibolite to be 420.2 ± 5.9 Ma and 430.3 ± 5.2 Ma, and the time period was Middle Silurian Epoch, which was consistent with the results of this age. Volcanic rocks are developed in the Lower Devonian Altenkos Formation outcropped in the Halke Mountain stratigraphic community, and their lithology is mostly basalt, which may be the source of early Devonian magmatic zircon. Liu B P et al. (1996) obtained an isotopic age of 282 ± 2 Ma ($^{40}Ar/^{39}Ar$ method) in the medium-acid volcanic rocks near 956 km of Duku Highway, which is consistent with the zircon harmonic age of 279.9 ± 6.8 Ma in the YSG-2 sample.

Li Z et al. (2004) inferred from the sandstone component model that the development of the source type of the Cenozoic “arc orogenic belt” in the Middle Cenozoic of the Kuqa depression is an indirect indication of the main curtain tectonic environment of the Late Paleozoic Tianshan orogenic orogenic structure. The provenance evolution of the Gidiq Formation and the tectonic uplift of the Tianshan Mountains are closely related to orogenesis. The zircon dating data of copper-bearing conglomerates of the Neophanic Gidike Formation (N_1j) in this paper show that the source mainly comes from the stratigraphy and magmatic rock products from the Late Silurian to the Early Permian in the Tianshan orogenic belt in the northwestern and southwest of the Kuqa Basin. It may be the result of denudation and redeposition of Late Silurian to Early Permian strata. At the same time, along with the denudation of existing copper deposits in the orogenic belt, the copper ore-forming elements also enter the Kuqa Basin, thus forming copper mineralization that spreads along the strata. The determinant of the scale of copper mineralization is determined by the supply of copper-forming minerals in the source area, that is, it is controlled by the size of the existing copper deposits (points) in the source area of the Tianshan Orogenic Belt in Southwest China, and the occurrence horizon is also limited by the time limit of the denudation and outcropping of the existing copper deposits (points), which in turn forms the mineral-bearing characteristics

of the Miocene Jidike Formation in the eastern part of the Kuqa Basin, and the mineral-bearing characteristics of the Kangcun Formation represented by the Dishui copper deposit in the western part of the Kuqa Basin.

Regionally, the area of Sarek—Urukchati—Ullagen—Sikel is a concentration area of large-medium conglomerate copper-lead-zinc deposits, represented by the Sarek Copper Deposit, Huayuan Copper Deposit and Jiashi Copper Deposit, and the Sarek Copper Deposit's ore-bearing horizon is Jurassic, The Cretaceous continuous sedimentary stratigraphy (Zhu X Y et al., 2011), the ore-bearing structure of the Sazheke copper deposit is the conglomerate of the Upper Jurassic Kuzhugongsu Formation (J_3k) and the purple conglomerate of the Lower Cretaceous Kizilsu Group (K_1kz), and the Tie Creek Copper Mine in Wensu County, the ore body is mainly hosted in the quartz sandstone of the Middle Devonian Kiziltao Formation (D_2kz) (Zhang C G et al., 2016). The Tamu-Kalangu lead-zinc belt is in the piedmont zone of the West Kunlun Mountains, and the deposits/occurrences occur in the carbonate rocks of the Upper Devonian-Lower Carboniferous platform (Zhu X Y et al., 2014). These deposits may have some potential connection to mineralisation in the study area in time and space.

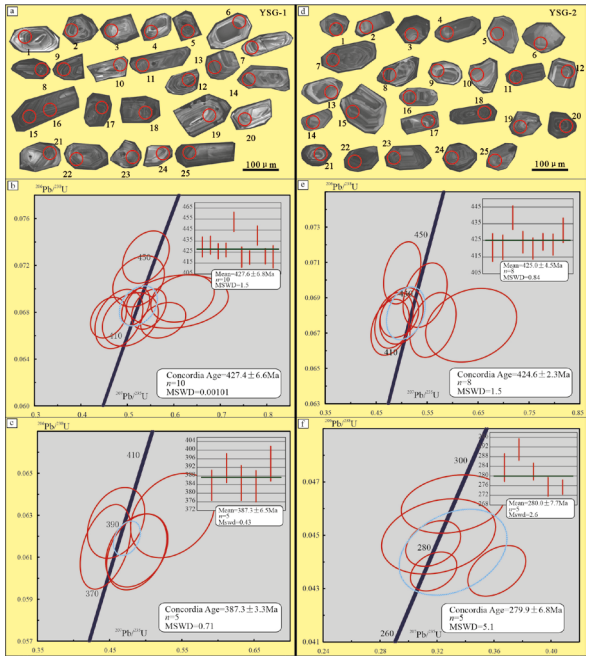

Figure 4. CL images, shrimp dating locations and results of pyroclastic zircons separated from sandstones of the Jidike Formation in the Yanshuigou area (a) CL image and shrimp dating locations of the sample YSG-1;(b,c)Dating results of the sample YSG-1; (d) CL image and Shrimp dating locations of the sample YSG-2; (e,f) Dating results of the sample YSG-2

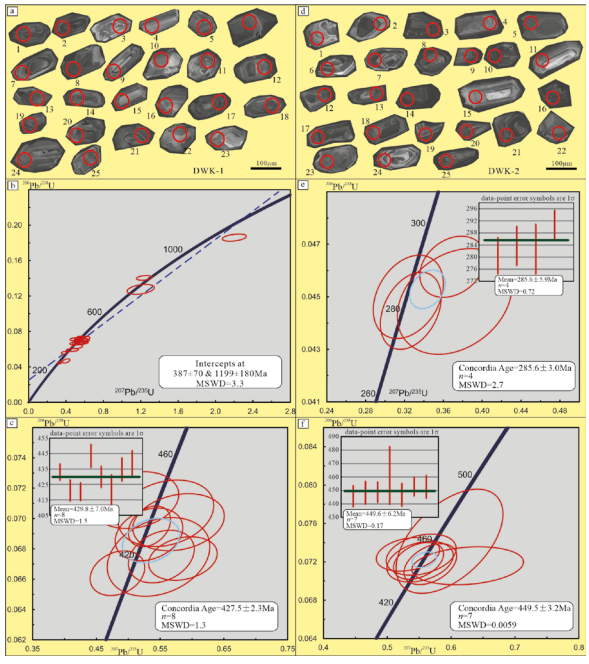

Figure 5. CL images, shrimp dating locations and results of pyroclastic zircons separated from sandstones of the Jidike Formation in the Duwanke area (a) CL image and shrimp dating locations of the sample YSG-1;(b,c)Dating results of the sample YSG-1; (d) CL image and Shrimp dating locations of the sample YSG-2; (e,f) Dating results of the sample YSG-2

Table2. Detrital zircon dating results of copper bearing conglomerate samples

Sample No	Total Pb	^{232}Th /10^{-6}	^{238}U /10^{-6}	$^{207}Pb/^{206}Pb$		$^{207}Pb/^{235}U$		$^{206}Pb/^{238}U$		$^{208}Pb/^{232}Th$		$^{238}U/^{232}Th$	$^{206}Pb/^{238}U$		Concordance
				Ratio	1σ	Ratio	1σ	Ratio	1σ	Ratio	1σ	Ratio	Age/Ma	1σ	
YSG-01-1	20.8285	153.7254	263.0202	0.06371	0.00758	0.60779	0.07227	0.06891	0.00150	0.01080	0.00148	1.06952	429.6	9.1	88%
YSG-01-2	24.4740	230.8566	287.6442	0.06511	0.00503	0.61869	0.04503	0.06919	0.00134	0.01073	0.00148	0.77831	431.3	8.1	87%
YSG-01-4	20.4037	174.3041	278.5160	0.05785	0.00348	0.48767	0.02840	0.06133	0.00115	0.00992	0.00147	1.00507	383.7	7.0	95%
YSG-01-5	41.5550	316.6094	524.6320	0.05787	0.00262	0.54628	0.02457	0.06827	0.00113	0.00919	0.00140	1.04387	425.7	6.8	96%
YSG-01-6	30.9223	192.0036	665.3373	0.05948	0.00358	0.35734	0.02151	0.04336	0.00084	0.00617	0.00102	2.22319	273.6	5.2	87%
YSG-01-7	31.0366	290.9565	411.4012	0.05294	0.00296	0.45895	0.02617	0.06264	0.00111	0.00804	0.00142	0.90878	391.6	6.8	97%
YSG-01-8	36.5193	329.2174	514.0955	0.05281	0.00282	0.44423	0.02313	0.06150	0.00133	0.00754	0.00146	1.08895	384.7	8.1	96%
YSG-01-9	50.0460	354.5938	628.5115	0.05505	0.00221	0.51795	0.01991	0.06847	0.00104	0.00777	0.00166	1.14019	426.9	6.3	99%
YSG-01-10	23.1054	190.3337	316.5864	0.05843	0.00346	0.48756	0.02751	0.06125	0.00119	0.00715	0.00170	1.11445	383.2	7.2	94%
YSG-01-11	22.9080	150.0174	434.0588	0.05285	0.00317	0.35063	0.02059	0.04821	0.00083	0.00475	0.00127	1.84286	303.5	5.1	99%
YSG-01-13	25.3246	219.8576	332.4841	0.06300	0.00502	0.53719	0.03845	0.06298	0.00133	0.00567	0.00192	0.95720	393.7	8.0	89%
YSG-01-14	22.3465	130.3364	273.6930	0.05412	0.00336	0.53987	0.03312	0.07271	0.00147	0.00755	0.00185	1.33333	452.5	8.9	96%
YSG-01-15	61.1415	233.4106	1234.011	0.05268	0.00198	0.34693	0.01360	0.04782	0.00067	0.00570	0.00121	3.29477	301.2	4.1	99%
YSG-01-16	33.8362	140.4038	666.2865	0.05335	0.00265	0.36061	0.01864	0.04912	0.00101	0.00619	0.00116	3.06602	309.1	6.2	98%
YSG-01-17	65.0650	404.4770	1326.623	0.06101	0.00274	0.37277	0.01908	0.04419	0.00081	0.00776	0.00132	2.05162	278.7	5.0	85%
YSG-01-18	45.1711	527.7261	1569.816	0.05806	0.00268	0.21007	0.01199	0.02645	0.00102	0.00601	0.00085	1.81770	168.3	6.4	85%
YSG-01-20	10.5178	79.2261	135.4577	0.05406	0.00394	0.50643	0.03970	0.06738	0.00151	0.01045	0.00124	1.07061	420.4	9.1	98%
YSG-01-21	26.3641	182.2929	336.5629	0.06207	0.00334	0.57717	0.03200	0.06731	0.00100	0.01082	0.00107	1.16127	420.0	6.0	90%
YSG-01-22	17.5392	148.0103	207.1738	0.05454	0.00385	0.52418	0.03667	0.07064	0.00144	0.01174	0.00108	0.86757	440.0	8.7	97%
YSG-01-23	17.6212	156.1241	222.3930	0.04981	0.00295	0.45928	0.02554	0.06754	0.00114	0.01087	0.00090	0.88176	421.3	6.9	90%
YSG-01-24	11.7000	98.3663	148.5230	0.05163	0.00323	0.48192	0.03407	0.06743	0.00167	0.01163	0.00094	0.93201	420.6	10.1	94%
YSG-01-25	31.2625	210.1370	602.7860	0.05329	0.00253	0.35022	0.01616	0.04789	0.00071	0.00818	0.00066	1.77758	429.6	9.1	98%
YSG-02-1	135.6158	134.9238	238.8641	0.15217	0.01127	9.60456	0.69011	0.45770	0.00608	0.02784	0.00792	1.14192	2429.4	26.9	98%
YSG-02-3	18.6289	120.0016	341.2743	0.05215	0.00426	0.35632	0.02821	0.04967	0.00089	0.00382	0.00105	1.80714	312.5	5.5	99%
YSG-02-4	15.9581	135.0896	318.1217	0.05226	0.00450	0.32111	0.02640	0.04496	0.00093	0.00331	0.00092	1.52299	283.5	5.7	99%
YSG-02-7	37.8181	236.6968	491.6646	0.06030	0.00324	0.56156	0.02997	0.06746	0.00121	0.00610	0.00182	1.33421	420.8	7.3	92%
YSG-02-8	23.9061	227.8884	451.4156	0.05176	0.00376	0.33111	0.02389	0.04617	0.00072	0.00401	0.00125	1.44708	291.0	4.4	99%
YSG-02-9	11.0276	84.3154	149.2452	0.06542	0.00619	0.56903	0.05509	0.06299	0.00172	0.00627	0.00206	1.14342	393.8	10.4	85%
YSG-02-10	10.8303	68.5124	128.7632	0.05613	0.00470	0.54203	0.04148	0.07122	0.00175	0.00805	0.00318	1.19998	443.5	10.5	99%
YSG-02-11	59.0621	386.3186	699.7288	0.05004	0.00237	0.50286	0.02217	0.07285	0.00110	0.00698	0.00243	1.18427	453.3	6.6	90%

(*Continued*)

Sample No	Total Pb	^{232}Th /10^{-6}	^{238}U /10^{-6}	$^{207}Pb/^{206}Pb$		$^{207}Pb/^{235}U$		$^{206}Pb/^{238}U$		$^{208}Pb/^{232}Th$		$^{238}U/^{232}Th$	$^{206}Pb/^{238}U$		Concordance
				Ratio	1σ	Ratio	1σ	Ratio	1σ	Ratio	1σ	Ratio	Age/Ma	1σ	
YSG-02-12	74.4245	289.8881	1495.384	0.05541	0.00209	0.36214	0.01323	0.04711	0.00052	0.00485	0.00176	3.29502	296.7	3.2	94%
YSG-02-13	70.9201	267.2635	1524.089	0.05119	0.00211	0.31736	0.01272	0.04469	0.00056	0.00512	0.00193	5.39146	281.8	3.5	99%
YSG-02-14	39.7020	114.6860	433.7612	0.05808	0.00227	0.69349	0.03082	0.08558	0.00187	0.01128	0.00286	2.41556	529.3	11.1	98%
YSG-02-15	20.4953	145.3932	253.7040	0.05175	0.00259	0.50119	0.02415	0.07041	0.00116	0.00909	0.00207	1.12960	438.6	7.0	93%
YSG-02-16	30.7933	304.5631	368.2499	0.05314	0.00305	0.49975	0.02814	0.06798	0.00106	0.00968	0.00197	0.79117	424.0	6.4	97%
YSG-02-17	33.8734	230.5634	705.7306	0.06032	0.00248	0.36201	0.01343	0.04367	0.00063	0.00715	0.00130	1.95668	275.5	3.9	87%
YSG-02-18	73.7846	464.2236	1574.102	0.05252	0.00179	0.31764	0.01075	0.04364	0.00048	0.00677	0.00110	2.23251	275.4	3.0	98%
YSG-02-19	21.7609	153.3115	276.7611	0.05122	0.00265	0.47748	0.02486	0.06733	0.00105	0.01184	0.00176	1.17061	420.0	6.3	94%
YSG-02-20	35.8555	339.6282	432.2324	0.05283	0.00278	0.49561	0.02497	0.06800	0.00082	0.01149	0.00154	0.81890	424.1	5.0	96%
YSG-02-21	33.7581	199.9798	521.3027	0.05919	0.00276	0.46544	0.02059	0.05722	0.00087	0.01236	0.00154	1.78310	358.7	5.3	92%
YSG-02-22	33.6318	275.5840	420.5644	0.05228	0.00282	0.48503	0.02491	0.06773	0.00105	0.01248	0.00142	0.98181	422.4	6.3	94%
YSG-02-23	24.3259	206.1028	291.5242	0.05757	0.00313	0.54606	0.02859	0.06915	0.00121	0.01305	0.00141	0.94164	431.0	7.3	97%
YSG-02-25	14.6843	57.8395	95.8393	0.06559	0.00472	1.16398	0.07744	0.13088	0.00321	0.02720	0.00278	1.08340	792.9	18.3	98%
DWK-1-1	40.0076	66.9948	190.7386	0.08598	0.00347	2.20170	0.08536	0.00267	0.37011	0.04041	0.00313	1.75041	1099.2	14.5	92%
DWK-1-2	41.2844	348.4192	496.3168	0.05574	0.00248	0.53324	0.02183	0.00089	0.31190	0.01355	0.00090	0.87637	433.1	5.3	99%
DWK-1-3	16.7200	87.2621	108.8454	0.07005	0.00649	1.19984	0.09620	0.00368	0.36026	0.02331	0.00167	0.76970	773.7	21.1	96%
DWK-1-4	12.7409	137.4739	165.2516	0.05987	0.00467	0.51832	0.04053	0.00144	0.29204	0.01240	0.00096	0.74202	393.7	8.7	92%
DWK-1-5	19.6103	128.9489	249.5879	0.05962	0.00396	0.55181	0.03409	0.00115	0.27476	0.01476	0.00111	1.20133	421.0	6.9	94%
DWK-1-6	26.2063	188.5719	537.6576	0.05354	0.00283	0.33192	0.01698	0.00082	0.35760	0.00931	0.00073	1.76579	281.8	5.0	96%
DWK-1-7	24.6173	241.5822	293.8625	0.06261	0.00403	0.58574	0.03550	0.00095	0.23195	0.01349	0.00110	0.77337	420.3	5.7	89%
DWK-1-8	33.3894	245.7539	444.6297	0.05218	0.00320	0.48305	0.02825	0.00097	0.25072	0.01174	0.00098	1.12532	414.4	5.9	96%
DWK-1-12	17.2754	137.4936	213.9984	0.05150	0.00476	0.51099	0.04498	0.00123	0.19694	0.01240	0.00140	0.95703	443.5	7.4	94%
DWK-1-13	20.7475	155.5542	309.8379	0.05654	0.00545	0.46774	0.04326	0.00107	0.19625	0.01143	0.00134	1.24995	370.1	6.5	94%
DWK-1-15	18.6070	109.0450	243.4941	0.05525	0.00384	0.53261	0.03502	0.00115	0.25306	0.01194	0.00153	1.39859	429.9	6.9	99%
DWK-1-16	10.3977	116.1228	123.0328	0.05898	0.00629	0.54753	0.05313	0.00171	0.26157	0.01111	0.00151	0.66279	420.9	10.3	94%
DWK-1-17	26.8469	199.7349	327.5278	0.05529	0.00386	0.54569	0.03477	0.00180	0.39200	0.01137	0.00162	1.04544	449.0	10.8	98%
DWK-1-18	26.6644	229.3990	304.7322	0.05566	0.00342	0.56258	0.03178	0.00101	0.24331	0.01168	0.00183	0.85556	455.5	6.0	99%
DWK-1-19	59.3480	126.4303	392.3663	0.06365	0.00316	1.23875	0.05577	0.00176	0.27898	0.02246	0.00368	1.96419	847.3	10.0	96%
DWK-1-21	13.9744	106.4127	173.4156	0.06074	0.00526	0.57891	0.04737	0.00124	0.21757	0.01187	0.00230	1.04310	434.7	7.5	93%
DWK-1-22	10.0480	92.0593	115.5757	0.06047	0.00505	0.58634	0.04559	0.00175	0.31366	0.01108	0.00246	0.78627	447.7	10.5	95%
DWK-1-23	10.6823	94.9507	130.5048	0.05857	0.00565	0.55910	0.04949	0.00145	0.23264	0.01191	0.00280	1.08103	438.2	8.7	97%
DWK-1-24	11.9333	86.3487	191.0244	0.05065	0.00347	0.38651	0.02423	0.00099	0.28232	0.00874	0.00214	1.41665	351.0	6.0	94%

(*Continued*)

Sample No	Total Pb	^{232}Th /10^{-6}	^{238}U /10^{-6}	$^{207}Pb/^{206}Pb$		$^{207}Pb/^{235}U$		$^{206}Pb/^{238}U$		$^{208}Pb/^{232}Th$		$^{238}U/^{232}Th$	$^{206}Pb/^{238}U$		Concordance
				Ratio	1σ	Ratio	1σ	Ratio	1σ	Ratio	1σ	Ratio	Age/Ma	1σ	
DWK-1-25	13.9142	107.2072	269.1796	0.06229	0.00420	0.40146	0.02684	0.00155	0.49481	0.00763	0.00208	1.58717	294.4	9.5	84%
DWK-02-1	10.2813	77.4032	134.0972	0.06023	0.00491	0.53373	0.04117	0.06584	0.00162	0.01061	0.00180	1.06254	411.1	9.8	94%
DWK-02-2	16.6663	100.3432	191.1727	0.05568	0.00322	0.58877	0.03282	0.07708	0.00188	0.01063	0.00170	1.17415	478.7	11.2	98%
DWK-02-3	41.8067	459.0936	801.7384	0.05290	0.00319	0.32651	0.02065	0.04447	0.00097	0.00699	0.00108	1.07514	280.5	6.0	97%
DWK-02-4	11.0689	105.8350	218.2531	0.05219	0.00377	0.32393	0.02380	0.04500	0.00105	0.00650	0.00101	1.28306	283.7	6.5	99%
DWK-02-5	19.7093	157.6658	291.2328	0.05348	0.00322	0.43221	0.02540	0.05840	0.00079	0.00862	0.00128	1.13361	365.9	4.8	99%
DWK-02-6	99.8021	360.0696	249.6272	0.10115	0.00335	3.93426	0.13338	0.27991	0.00385	0.03682	0.00535	0.43530	1590.9	19.4	98%
DWK-02-7	36.3444	478.3603	615.4290	0.05467	0.00333	0.36778	0.02074	0.04894	0.00092	0.00645	0.00095	0.81721	308.0	5.7	96%
DWK-02-8	24.4951	175.1110	298.1691	0.06299	0.00567	0.62590	0.05773	0.07159	0.00131	0.00937	0.00151	1.09391	445.7	7.9	89%
DWK-02-9	16.5471	128.6940	197.4754	0.05531	0.00356	0.55134	0.03430	0.07201	0.00140	0.00946	0.00150	0.94177	448.3	8.4	99%
DWK-02-10	29.6659	243.7200	348.1533	0.05525	0.00275	0.54889	0.02589	0.07210	0.00127	0.00902	0.00146	0.91370	448.8	7.6	98%
DWK-02-11	6.7809	64.1087	133.7215	0.06162	0.00668	0.37158	0.03893	0.04482	0.00133	0.00605	0.00111	1.30066	282.7	8.2	87%
DWK-02-12	20.9687	170.5373	269.2972	0.05621	0.00333	0.52333	0.03000	0.06747	0.00136	0.00761	0.00140	0.97748	420.9	8.2	98%
DWK-02-13	18.7532	168.1269	358.3538	0.05808	0.00370	0.36931	0.02213	0.04614	0.00077	0.00598	0.00119	1.32145	290.8	4.7	90%
DWK-02-14	68.1741	85.7095	491.3326	0.06361	0.00251	1.20141	0.04792	0.13550	0.00196	0.01660	0.00273	3.57799	819.2	11.1	97%
DWK-02-15	10.1311	69.1219	121.3937	0.06185	0.00643	0.59750	0.05521	0.07414	0.00358	0.00969	0.00162	1.08977	461.1	21.5	96%
DWK-02-16	39.9848	258.8460	461.6494	0.05532	0.00270	0.58379	0.02610	0.07653	0.00145	0.01023	0.00144	1.10860	475.4	8.7	98%
DWK-02-17	18.3521	176.3820	346.8909	0.05234	0.00683	0.34688	0.04344	0.04856	0.00109	0.00586	0.00081	1.21896	305.6	6.7	98%
DWK-02-19	28.3288	218.7605	341.0527	0.05757	0.00295	0.56744	0.02725	0.07176	0.00141	0.01082	0.00134	0.97078	446.7	8.5	97%
DWK-02-20	19.5768	185.9476	282.8082	0.06087	0.00407	0.49888	0.03210	0.05948	0.00169	0.00912	0.00118	0.95523	372.5	10.3	90%
DWK-02-21	22.4843	178.1707	267.3710	0.05272	0.00334	0.53241	0.03274	0.07278	0.00115	0.01100	0.00137	0.93547	452.9	6.9	95%
DWK-02-22	18.5524	109.3226	233.2820	0.05443	0.00344	0.55312	0.03618	0.07275	0.00141	0.01120	0.00144	1.32338	452.7	8.5	98%
DWK-02-23	22.5734	173.9300	251.9063	0.05622	0.00417	0.60333	0.04504	0.07727	0.00187	0.01337	0.00172	0.90692	479.8	11.2	99%
DWK-02-24	13.0107	48.8861	159.9213	0.06088	0.00498	0.65023	0.05559	0.07777	0.00247	0.01667	0.00232	2.07938	482.8	14.8	94%
DWK-02-25	20.5329	80.8152	246.6632	0.05283	0.00317	0.58276	0.03405	0.07978	0.00175	0.01284	0.00178	1.92111	494.8	10.5	94%

Note: data missing due to invalid zircon measurement points.

4 Conclusions

(1) The main sedimentary facies types can be identified in the Neogene in the southeast Kuqa foreland basin of Xinjiang, which are alluvial fan facies, fan-delta facies and lake facies, and further 5 subfacies and 7 microfacies types can be identified. In terms of genesis, sandstone-type copper mineralization is closely related to the Neogene fluvial-lacustrine sedimentary environment, and the minerals are mainly distributed in the fan-delta plain facies and fan-delta front facies.

(2) The detrital zircon dating data show that the copper-bearing conglomerates in the Miocene Jidike Formation (N_1j) in the southeast of the Kuqa Basin mainly come from the strata and magmatic rock products from the Late Silurian to the Early Permian in the northern and southwestern Tianshan orogenic belt in the north and southwest of the Kuqa Basin, which are the result of redeposition after strata denudation.

References

CAI H A, GAO H O, FAN S J, et al., 2022. The metallogenic model of the sandstone-type copper deposits in the Kangcun area, Kuqa Basin, Xinjiang [J]. Journal of Geomechanics, 28(1): 78-89. (in Chinese with English abstract)

CAI H A. 2023. Provenance analysis of sandstone type copper deposits in Kangcun area, Kuqa Basin, Xinjiang, China: LA-ICP-MS zircon U-Pb dating[J]. Mineral Exploration,14(11): 2032-2038.

CAO Y T. 2010. Development and regularity of evaporates and its metallization in Kuqa basin from Paleogene to Neogene[D]. Beijing: Chinese Academy of Geological Sciences: 1-158. (in Chinese with English abstract)

CAO Y T, LIU C L, CHEN Y Z, et al. 2010. Characteristics of copper mineralization in the Kuqa foreland basin, and origin, enrichment and distribution of copper[J]. Acta Geologica Sinica, 84(12): 1791-1804. (in Chinese with English abstract)

CHARREAU J, GILDER S, YAN C, et al. Magnetostratigraphy of the Yaha section, Tarim Basin (China): 11 Ma acceleration in erosion and uplift of the Tian Shan Mountains[J]. Geology, 2006, 34(3). DOI:10.1130/022106.1.

FANG W X, JIA R X, GUO Y Q, et al. 2016. Hydrocarbon-rich basin fluid with reductibility and metallogenic mechanism for glutenite-type Cu-Pb-Zn-U deposits in the western of Tarim basin[J]. Journal of Earth Sciences and Environment, 38(6): 727-752. (in Chinese with English abstract)

GUAN S W,CHEN Z X,LI B L,et al. 2010. Discussions on the character and interpretation model of Kelasu deep structures in the Kuqa area[J]Petroleum Exploration and Development,37(5):531-536.

GUO X P, DING X Z, HE X X, et al. 2002. New progress in the study of marine transgressional events and marine strata of the Meso-Cenozoic in the Tarim basin[J]. Acta Geologica Sinica, 76(3): 299-307. (in Chinese with English abstract)

HU B,ZHAI M G,PENG P, et al. 2013. Late Paleoproterozoic to Neoproterozoic geological events of the North China Craton: Evidences from LA-ICP-MS U-Pb geochronology of detrital zircons from the Cambrian and Jurassic sedimentary rocks in Western Hills of Beijing. Acta Petrologica Sinica,29(7) : 2508-2536. (in Chinese with English abstract)

JIA C Z, WEI G Q, YAO H J, et al. 1995. Tectonic evolution and regional structural geology[M]. Beijing: Petroleum Industry Press. (in Chinese)

LI J F, ZHAO Y, PEI J L, et al. 2017. Cenozoic marine sedimentation problem of the Tarim basin[J]. Journal of Geomechanics, 23(1): 141-149. (in Chinese with English abstract)

LI S J, SHI Y H, WANG Q C, 2006. The analysis of detrital heavy minerals in Cretaceous-Tertiary sandstones, Kuqa Depression and their implications for provenance[J]. Acta Sedimentologica Sinica, 24(1): 28-35. (in Chinese with English abstract)

LI X, ZHONG D K, LI Y, et al. 2013. Sedimentary characteristics and evolution of the Neogene and Quaternary in Kuqa Depression of Tarim Basin[J]. Journal of Paleography, 15(2): 169-180. (in Chinese with English abstract)

LI Z, WANG D X, LIN W, et al. 2004. Mesozoic-Cenozoic clastic composition in Kuqa depression, northwest China: implication for provenance types and tectonic attributes[J]. Acta Petrologica Sinica, 20(3): 655-666. (in Chinese with English abstract)

LIN C S, LIU J Y, ZHANG Y M, et al. 2002. Characteristics of tertiary structural sequence and its response to foreland tectonism in Kuqa depression[J]. Science in China (Series D), 32(3): 177-183. (in Chinese)

LIU B P, WANG Z Q, ZHANG C H, et al. 1996. Tectonic framework and evolution in southwest Tianshan mountains,China[M]. Wuhan: China University of Geosciences Press: 1-120. (in Chinese)

LIU D Q, TANG Y L, ZHOU R H. 2005. Copper deposits and nickel deposits in Xinjiang, China[M]. Beijing: Geological Publishing House: 171. (in Chinese)

LIU Z H, LU H F, LI X J, et al. 2000. Tectonic evolution of Kuqa rejuvenated foreland basin[J]. Scientia Geologica Sinica, 35(4): 482-492. (in Chinese with English abstract)

LU K G, WANG G R, SUN X. 2019. Interlayered oxidation-zone styles in fault-fold belts of the northern Tarim basin and its controlling to the formation of sandstone-type uranium deposits[J]. Journal of Geomechanics, 25(1): 115-124. (in Chinese with English abstract)

QIAN J F, XIAO A C, YANG S F. 2012. Research on mesozoic-cenozoic structural characteristics and evolution in northwestern margin,Tarim basin[M]. Hangzhou: Zhejiang Business University Press: 1-128. (in Chinese)

QIU F Q, DING Y, WANG H. 2000. Source analysis on deposits of Kuche basin[J]. Xinjiang Geology, 18(3): 252-257. (in Chinese with English abstract)

SHAO L Y, HE Z P, GU J Y, et al. 2006. Lithofacies palaeogeography of the Paleogene in Tarim Basin[J]. Journal of Palaeogeography, 8(3): 353-364. (in Chinese with English abstract)

SHAO L Y, LUO W L, GU J Y, et al. 2007. A basin-wide sequence stratigraphic analysis of the Paleogene in Tarim Basin[J]. Journal of Palaeogeography, 9(3): 283-292. (in Chinese with English abstract)

SHI W G,GONG E P, CHU Y G, et al. 2015. Sedimentary system and depositional environment of copper-bearing rock series of Neogene in Baicheng County,Xinjiang. Acta Sedimentologica Sinica, 33(06):1074-1086. (in Chinese with English abstract)

TAN X C, WANG Z Y, LI L, et al. 2006. Arrangement and evolution of Tertiary sedimentary facies in Kuche foreland basin, Xinjiang[J]. Acta Sedimentologica Sinica, 24(6): 790-797. (in Chinese with English abstract)

TANG L J, JIA C Z, PI X J, et al. 2004. Salt-related structural styles of Kuqa foreland fold belt, northern Tarim basin. Science in China(D), 47(10): 886-895.

TIAN Z J, SONG J G, 1999. Tertiary structure characteristics and evolution of Kuche foreland basin[J]. Acta Petrolei Sinca, 20(4): 7-13. (in Chinese with English abstract)

WU F L, YAO Z G. 2011. Application of U-Pb dating in the study on the provenance analysis of detrital zircons in the southern margin of Junggar Basin,China. Journal of Xi'an Shiyou University (Natural Science Edition), 26(03): 6-13. (in Chinese with English abstract)

XIAO Y, 2018. Tectono-thermal evolution of northern Kuqa Depression and South Tien Shan[D]. Beijing: China University of Petroleum (Beijing): 1-88. (in Chinese with English abstract)

YAN F L, LU H F, JIA D, et al. 2003. The Meso-Cenozoic subsidence features of Kuqa Depression, Tarim Basin[J]. Journal of Nanjing University (Natural Sciences), 39(1): 31-39. (in Chinese with English abstract)

YANG G, QIAN X L, 1995. Subsidence of the Kuqa depression and Mesozoic-Cenozoic structural reactivations in Tianshan[J]. Xinjiang Geology, 13(3): 264-274. (in Chinese with English abstract)

ZHANG C G, LAI J Q, CAO Y H. et al., 2016. Polygenetic compound mineralization of Tiekelike copper-lead-zinc deposit, Xinjiang [J]. The Chinese Journal of Nonferrous Metals, 26(6): 1293−1302.

ZHANG M L, TAN C X, TANG L J, et al. 2004. An analysis of the Mesozoic-Cenozoic tectonic stress field in Kuqa depression, Tarim Basin[J]. Acta Geoscientica Sinica, 25(6): 615-619. (in Chinese with English abstract)

ZHANG T, CHEN Z L, HUANG H Y, et al. 2020, Geochemical characteristics of gold-bearing minerals and its geological significance in the Ashawayi gold deposit in the southwestern Tianshan Orogen[J]. Journal of Geomechanics, 26 (3): 443-458. (in Chinese with English abstract)

ZHAO M J, LU X S, ZHUO Q G, et al. 2015. Characteristics and distribution law of hydrocarbon accumulation in Kuqa foreland basin[J]. Acta Petrolei Sinica, 36(4): 395-404. (in Chinese with English abstract)

ZHU X Y, WANG J B, 2014. Study on metallogenic system of Pb-Zn, Cu and U deposits associated with basin brines in the southwestern Tarim basin, Xinjiang[J]. Mineral Exploration, 5(2): 136-148. (in Chinese with English abstract)

ZHU X Y,WANG J B,WANG Y J, et al. 2011. The geologic characteristics of sareke copper deposit,Xinjiang,China——ore genesis related to basin brines[J]. Mineral Exploration, 2(1): 28−35. (in Chinese with English abstract)